

LBL--13820

DE82 012794

**PRE-PRECIPITATION PHENOMENA AT GRAIN BOUNDARIES**

**J. Briceno-Valero and R. Gronsky**

**Materials and Molecular Research Division**

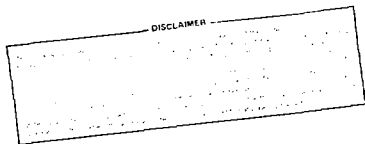
**Lawrence Berkeley Laboratory**

**and**

**Department of Materials Science and Mineral Engineering**

**University of California**

**Berkeley, CA 94720**



NOTICE

ALL INFORMATION CONTAINED HEREIN IS UNCLASSIFIED EXCEPT WHERE SHOWN OTHERWISE

DATE 11-19-82 BY SP-1/STW/STW

THIS DOCUMENT IS UNCLASSIFIED

### Abstract

A high spatial resolution study of the behavior of Zn solute in Al bicrystals has been conducted using x-ray energy-dispersive spectroscopy (EDS) in a TEM/STEM instrument. Specimens subjected to short annealing cycles are found to exhibit a periodic distribution of Zn along the grain boundary plane prior to the appearance of any evidence suggesting precipitation has occurred. The periodicity of the segregation event bears no exact relationship with the transition lattice models of boundary structure but its behavior as a function of misorientation angle does agree with the expected intervals of atomic relaxation in the O-lattice. High resolution images and convergent beam microdiffraction are used to confirm the structural characteristics of these solute-rich regions.

### Introduction

Studies of the relationship between grain boundary structure and grain boundary precipitation have shown (1) that there is a profound effect of local atomic structure upon the emergence and development of second phase particles at grain boundaries. In particular, unless the grain boundary plane is a suitable low-index habit plane for the new phase, then precipitation is favored at the site of defects within the actual boundary region. Such site specificity is highly localized and is indicated to be a strong influence at the nucleation stage of grain boundary reactions (1).

The present investigation began as an attempt to determine the exact relationship between grain boundary structure and the nucleation event in these reactions. The results reported here pertain to solute segregation phenomena which actually precede nucleation in specimens of controlled grain boundary geometry. The spatial distribution of Zn at grain boundaries in Al bicrystals has been monitored by TEM imaging coupled with STEM microanalysis in order to determine the specific association between Zn concentration and grain boundary structure.

### Experimental Procedure

Bicrystals of 99.999% Al were prepared by a modified Czochralski method using two oriented seed crystals. After slicing to expose the boundary plane perpendicular to the sample surface, a layer of Zn was vacuum evaporated onto the specimens and subjected to a diffusion anneal. The coated discs were encapsulated in argon-filled quartz tubing prior to heat treatment at 500°C for various times. Residual surface films were removed and 3mm diameter discs were cut from the grain boundary area. Transmission electron microscope (TEM) specimens were then prepared by jet electropolishing in a solution of 1 part nitric acid, 3 parts methanol at -30°C. After thinning, the foils were washed repeatedly in distilled water, methanol and ethanol (in that order) to minimize the occurrence of specimen-borne contamination build-up in the microscope environment.

The specimens were examined in a Philips EM400 TEM with scanning transmission (STEM) attachment and energy dispersive x-ray spectrometer. The microscope was operated at an accelerating potential of 100kV, using a pointed LaB<sub>6</sub> filament and a beam current of approximately 10 microamps. A focused beam diameter of 4nm was utilized in the STEM mode, and standard precautions (low background holder, high take-off angle) were taken to optimize the x-ray signal.

A chemical profile was obtained by placing the probe at successive intervals of a few hundred angstroms along the grain boundary plane for a total distance of a few microns. In order to overcome the problems of foil thickness variations, only those boundaries which ran parallel to the edge of the perforation were analyzed, using a working STEM magnification of approximately 100,000X. For all boundaries, thickness measurements were nevertheless taken by convergent beam electron diffraction, and the axis/angle pair description of every boundary was determined by conventional diffraction analysis.

For quantitative compositional analyses, the effects of beam divergence in the boundary vicinity have been acknowledged (2); however, in most instances, the parameter of interest was the qualitative ratio of count rates (3) for the binary elements Zn and Al.

Following the analytical profiles, all boundary regions were imaged by high resolution weak beam and conventional methods. Correlations were then sought between all compositional and structural data.

### Experimental Results

A summary plot of the composition profiles along three different grain boundaries is presented in Fig. 1. The boundaries are identified according to their nearest coincidence site lattice (CSL) (5) for purposes of classification, with Zn/Al count rate ratio plotted as a function of distance along the grain boundary plane. As reflected in this particular example, it was found that as the density of coincidence sites in the transition lattice increased, the ability to locate isolated solute-rich regions decreased. Note that for the  $\Sigma = 17$  boundary shown here, the concentration profile along the boundary plane appeared absolutely flat.

By comparison, the low  $\Sigma$  boundaries not only showed clearly-defined solute pockets, but these solute-rich regions appeared to be periodically distributed along the boundary as well. For this feature, however, the CSL model proved too general a categorization scheme. The two  $\Sigma = 7$  boundaries depicted here show obvious variations in the "wavelength" of the periodic profiles: the spacing of the boundary with a  $\langle 111 \rangle$  rotation axis is roughly 300nm while that of the boundary with a  $\langle 311 \rangle$  rotation axis is about 200nm, even though they have the same density of coincidence points in the transition lattice.

Composition peaks indicating high Zn regions were detected along numerous boundaries where high resolution imaging failed to indicate any second phase particles. All peaks were clearly defined, with error bars on Fig. 1 indicating the global

experimental uncertainties. Typically the Al  $K_{\alpha}$  x-ray signal contained about  $10^4$  counts while the Zn  $K_{\alpha}$  signal topped off at about 2500 counts when using a 230eV energy window and 150 second minimum count time. Background readings on either side of these signals rarely reached 400 counts.

Further attempted correlations between the structural aspects of the grain boundary plane and the segregation events did yield results relating to ledge behavior as shown above. Figure 2 is a bright field image of a rather large ledge in one of the low bicrystal boundaries. The results of an EDS probe of areas 1, 2, and 3 yielded the peaks shown in Fig. 3, for a rather large (40nm) probe diameter. After background stripping, the integrated peaks showed a higher Zn concentration on the large grain boundary step with somewhat less Zn at the flat, planar portions of the boundary. The lowest peak in Fig. 3 comes from region 3 of the adjacent matrix and the overlapping Cu signal attests to the accuracy of the relative Zn peak heights. Similar point probes on smaller ledges were attempted, but the signal to noise ratio in these studies fell into the uncertain range.

### Discussion

The interesting aspect of the observed periodic nature of Zn segregation in the Al bicrystals studied here is that it indicates a strong tendency for preferential solute clustering along the boundary plane. Unfortunately, the precise identification of the character of such sites remains ambiguous. The obvious lack of any meaningful relationship between the periodicity of preferred sites and the nearest CSL rules out intrinsic grain boundary structures as a determining factor. However, depending upon the proximity to an exact coincidence relationship, there is some agreement between the large scale of the segregation periodicity (>100nm) and the large scale relaxations in boundary structure expected for minute deviations from an exact  $\Sigma$  boundary. These relaxation events, more accurately described using an O-lattice model (4), can in fact take on values of mean separation in the 100nm range. Nevertheless, there

are severe difficulties in detecting these defect structures, both due to their small strain fields and due to the practical complications caused by specimen contamination under a finely-focused electron probe.

It is far more evident that extrinsic structures do influence the pattern of grain boundary segregation from the results in Figs. 2 and 3. The tendency for large ledges in particular to accumulate more solute is not surprising given the dual nature of that particular heterogeneity with respect to surface and strain energy reduction. Convergent beam diffraction patterns from the ledge regions in fact indicate some lattice distortion which is not present at the planar boundary regions. There is also some question concerning whether or not the solute doping treatment actually caused ledge formation, i.e. that the ledges were formed to accommodate excess solute. An examination of undoped bicrystals from the same ingot showed no such boundary structure. Unfortunately, the presence of ledges could have been induced purely by thermal activation, and the annealing experiments to test this possibility are currently underway.

The hierarchy of structural influences on segregation for the specific boundaries studied here is in exact agreement with that of grain boundary precipitation for similar alloy systems (1). The domination of extrinsic boundary structures and subtle role of intrinsic structural units as well favors the point of view that local conditions of equilibrium or local departure from equilibrium is achieved because of favorable boundary structure. This is not contradicted by the possibility that segregation itself may induce changes in the character of extrinsic defects within the boundary plane. The point is that periodic solute enrichment was not observed for all boundaries, therefore a boundary must possess an appropriate structure to be able to accommodate extra solute, and it may do so by local structural adjustments.

Finally, it is pointed out that the levels of solute doping used in this study were intentionally high, chiefly to avoid the limitations imposed by the experimental

techniques. Present and future experiments have been designed to use lower initial solute levels, polycrystals, and time evolution studies for assessment of the full transition to a grain boundary phase.

This work was supported by the Director, Office of Energy Research, Office of Basic Energy Sciences, Materials Science Division of the U. S. Department of Energy under contract No. DE-AC03-76SF00098.

1. R. Gronsky and P. Furrer, *Met. Trans.* 12A, 121 (1981).
2. P. Doig and P. E. J. Flewitt, *J. Microscopy* 110, 107 (1977).
3. J. Briceno-Valero and R. Gronsky, in 38th Ann. Proc. Electron Microscopy Soc. Amer., G. W. Bailey (ed.), Claitors's, Baton Rouge, p. 360 (1980).
4. W. Bollmann, Crystal Defects and Crystalline Interfaces, Springer-Verlag, New York (1970).

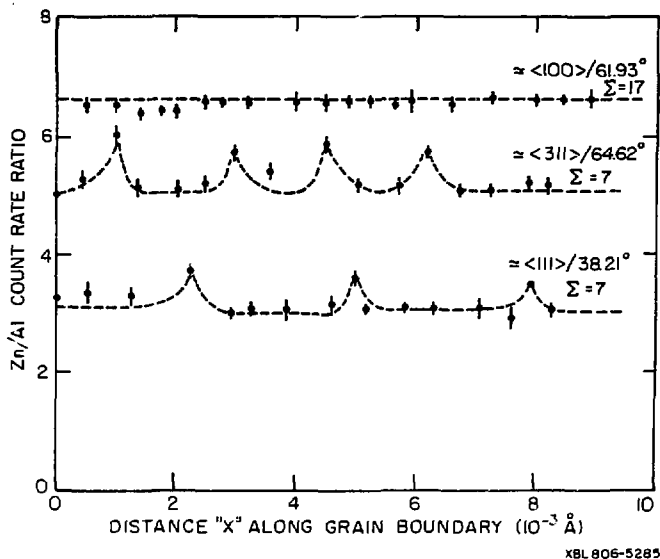
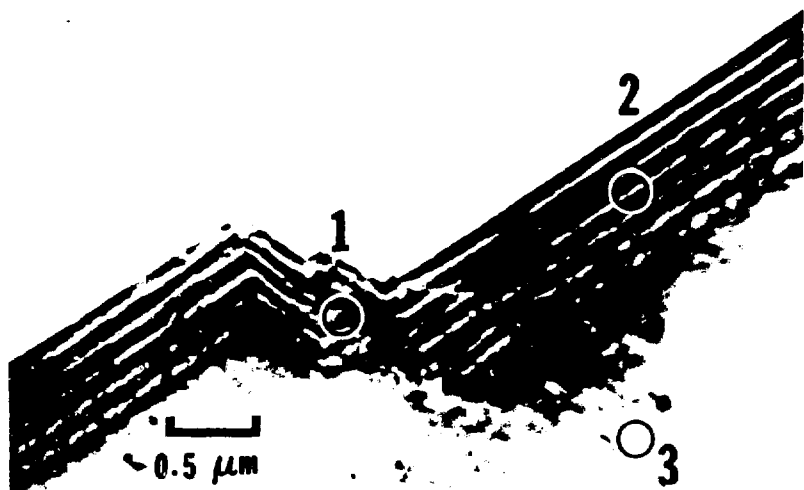


Fig. 1. Plot of the Zn/Al count rate ratio as a function of distance along the boundary plane for three bicrystals, classified according to their axis/angle pair.





XBE 817-F572

Fig. 2. TEM image of a low  $\epsilon$  boundary showing large central ledge structure. The numbered regions correspond to Fig. 3.

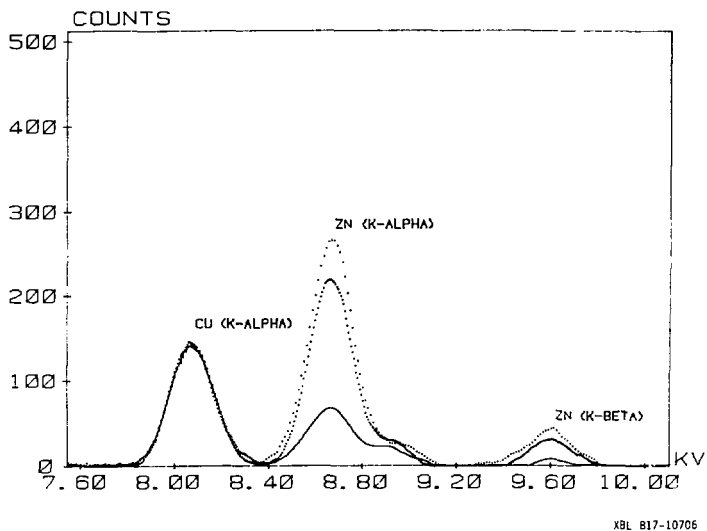


Fig. 3. EDS output for the regions of Fig. 2. The high Zn signal is from the ledge region 1, the intermediate from boundary region 2 and the low from matrix region 3.